EasyChair Preprint

№ 10969

Super Twisting Sliding Mode Control of a Robotic Manipulator Actuated by Shape Memory Alloy: Design and Experiment

Mohammad Mohammadi Shahir, Mehdi Mirzaei, Sadra Rafatnia and Zahra Ahangari Sisi

September 26, 2023

Super twisting sliding mode control of a robotic manipulator actuated by shape memory alloy: Design and experiment

1st Mohammad Mohammadi Shahir
Faculty of Mechanical Engineering
Sahannd University of Technology
Tabriz, Iran
mi.shahir74@gmail.com

2nd Mehdi Mirzaei
Faculty of Mechanical Engineering
Sahannd University of Technology
Tabriz, Iran
mirzaei@sut.ac.ir

3rd Sadra Rafatnia
Faculty of Mechanical Engineering
Sahannd University of Technology
Tabriz, Iran
sa_rafatnia@sut.ac.ir

4th Zahra Ahangari Sisi
Faculty of Mechanical Engineering
Sahannd University of Technology
Tabriz, Iran
z_ahangari98@sut.ac.ir

***Abstract*—This study focuses on practical implementation of a robust nonlinear controller, designed for a robotic manipulator under actuation of shape memory alloy (SMA). The nonlinear behavior of SMA, due to hysteresis effects, brings a complexity to the mathematical model of the robotic system, resulting in an increase of its degree of freedom. To address this issue, a reduced-order model is employed for designing the controller. However, the effect of un-modeled dynamics is compensated by a super twisting sliding mode control because of its capability in dealing with uncertainty. The simulation and experimental results indicate robust performance for the proposed controller in tracking different trajectories specified for the robotic manipulator. Moreover, in comparison with the traditional sliding model control, the proposed method has higher tracking accuracy with less chattering in the presence of model uncertainties.**

***Index Terms*—Shape memory alloy, Robotic manipulator, super twisting sliding mode control, Model reduction.**

I. Introduction

Shape memory alloys (SMAs) have played a crucial role in scientific and industrial applications due to their remarkable capacity to return to their initial shape when exposed to specific thermal energies [1]. Various factors such as light weight, portable size, rapid response, and minimal noise enable SMAs to become significantly useful in medical equipment [2], [3], robotic [4], [5], and automotive vehicle parts [6]. However, one of the drawbacks of SMAs used as systems actuator is their nonlinear behavior due to the hysteresis effect, which causes delays in the performance of the systems [7], [8]. These limitations cause slow responses and make difficulties in designing accurate and precise motion controllers [9].

Several approaches have been proposed to increase the performance of the position controller for systems actuated with SMA. The methods are typically based on developing mathematical models to accurately describe the hysteresis effects, or designing the controllers with the ability of compensating for uncertainties in the system [10].

The behavior of SMAs can be described based on mathematical models such as the Liang model [11]–[13], the Duhem model [7], [13], and other empirical models [14], [15]. However, using these mathematical modeles for design of the controllers may be challenging because of their high degree of freedoms, resulting in an increased relative degree between the input and output of the system. For this reason, Tai et al. [16] introduced a reduced-order mathematical model to decrease the complexity of the mathematical model of SMA [17]. However, the un-modeled dynamics brings uncertainty to the models, making challenges for the control systems.

Among various controllers used to reject model uncertainties [1], [10], Sliding Mode Control (SMC) is one of the most practical and useful methods in the field of nonlinear control [18]. The main feature of SMC is its robustness against model uncertainty and unknown disturbances [7], [19]. This feature enables the SMC to be used in various applications [20]. However, the main drawback of SMC is the chattering phenomenon, leading to a negative impact on control accuracy and may contribute to the instability of the control system [21], [22]. To overcome these difficulties, several approaches have been proposed in the literature. One method is super-twisting sliding mode control (ST-SMC), characterized by the ability to reduce the chattering phenomenon. This method has a more robustness against uncertainties and disturbances, and is able to transfer the state of the system to the equilibrium point within a finite time frame [23], [24].

In this article, a ST-SMC is designed and implemented for position control of a robotic manipulator actuated by SMA. A reduced-order model with 1-DOF is employed for the controller design. In order to assess the effectiveness of the control method, an experimental platform equipped with an

SMA actuator is provided for controlling the position of the manipulator. The performance of the proposed controller is evaluated across various trajectories. The results show that the proposed strategy, compared with traditional SMC, has higher performance and accuracy in tracking the desired trajectory in the presence of un-modeled dynamics.

The paper is organized as follows: In Section II, The nonlinear dynamic model of SMA is presented. In Section III-B, the proposed control method is developed and analyzed. Then, the proposed control method is evaluated through simulation and experimental studies in Section IV. Finally, the conclusion is drawn in Section V.

II. The Overview of the Proposed Control System

Figure 1 illustrates the structure of the platform consisting of a robot manipulator actuated by SMA. A two-phase encoder is used to measure the angular displacement of the arm. Additionally, a serial connection is established between the platform and the MATLAB software for the processing of the proposed control method. Finally, the control signal generated by the proposed method is sent to the SMA actuator via a serial port to complete the hardware-in-the-loop structure.

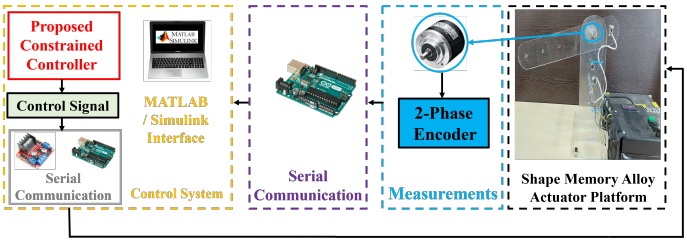

Fig. 1. The schematic of the SMA actuated position control system.

III. Design of Control System

A. Dynamic Modeling

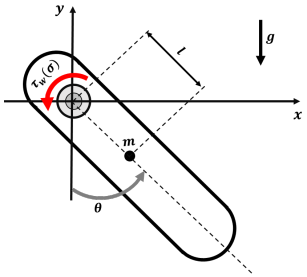

Fig. 2. Schematic diagram of robot arm

According to Fig. 2, the governing equation of motion for the link is derived using Newton's second law, expressed as follows [25]:

$$I_z\ddot{\theta} + c\dot{\theta} + k\theta + mglcos\theta = \tau_w(\sigma), \tag{1}$$

where θ represents angular displacement, I_z is rotational inertia, m is the mass of the arm, g is the gravitational acceleration, l is the distance from the center of mass, k is the torsion spring constant, and c represents the torsional damping coefficient. Finally, $\tau_w(\sigma)$ represents the torque generated by the SMA wire.

The constitutive model of the wire, which defines the relationship between stress rate $\dot{\sigma}$, strain rate $\dot{\epsilon}$, martensite fraction rate $\dot{\eta}$, and temperature rate $\dot{T}$, is defined as follows [26]:

$$\dot{\sigma} = \theta_T\dot{T} + \Omega\dot{\eta} + D\dot{\varepsilon}, \tag{2}$$

where θ_T is the thermal expansion factor, Ω is the phase transformation contribution factor, and D is the average Young modulus. The mathematical formulation for temperature is defined as follows:

$$\dot{T} = \frac{1}{m_w c_p}[\frac{V^2}{R} - h_c A_s(T - T_\infty)], \tag{3}$$

where V is the voltage applied to the wire, m_w represents the mass per unit length of the wire, c represents the specific heat of the wire, R signifies the resistance of the wire, A_s represents the surface area of the wire, and h_c represents the heat transfer coefficient. Finally, T and T_∞ represent the temperature and the ambient temperature of the wire, respectively.

The hysteresis behavior of SMA during heating and cooling causes nonlinear phase transformation equations. In this article, Liang's model [26] is used to define equations of phase transformation during cooling and heating. The phase transformation during heating is described as follows:

$$\eta_{(M\to A)} = \frac{\eta_M}{2}\left(\cos\left[a_A(T - A_S) + b_A\sigma\right] + 1\right), \tag{4}$$

where $a_A = \frac{\pi}{(A_f - A_s)}$, $b_A = -\frac{a_A}{C_A}$. In this model, $\eta_{(M\to A)}$ represents the phase transformation from Martensite phase M to Austenite phase A. The variable η_M represents the initial Martensite fraction. A_s and A_f represent the start and final temperatures of the Austenite phase and C_A is the curve fitting parameter.

On cooling, the phase of SMA transforms from Austenite to Martensite. The phase transformation during cooling is described as

$$\eta_{(A\to M)} = \frac{1 - \eta_A}{2}\left(\cos\left[a_M(T - M_f) + b_M\sigma\right] + 1\right) + \frac{1 + \eta_A}{2}, \tag{5}$$

where $a_M = \frac{\pi}{(M_f - M_s)}$, and $b_M = -\frac{a_M}{C_M}$. In this model, $\eta_{(A\to M)}$ represents the phase transformation from Austenite phase to Martensite phase . The variable η_A represents the initial Austenite fraction. M_s and M_f represent the start and final temperatures of the Martensite phase and C_M is the curve fitting parameter.

By deriving from Eq. (4), the martensite fraction rate for heating is described as

$$\dot{\eta}_{(M\to A)} = -\frac{\eta_m}{2}\sin[a_A(T - A_S) + b_A\sigma][a_A\dot{T} + b_A\dot{\sigma}], \tag{6}$$

The condition for the phase transformation from Martensite to Austenite is expressed as

$$A_f + \frac{\sigma}{C_M} < T < A_s + \frac{\sigma}{C_M}. \tag{7}$$

The martensite fraction rate for cooling is obtained from Eq. (5) as

$$\dot{\eta}_{(A\to M)} = -\frac{1-\eta_A}{2}\sin[a_M(T-M_f)+b_M\sigma][a_M\dot{T}+b_M\dot{\sigma}]. \tag{8}$$

The condition for the phase transformation from Austenite to Martensite is expressed as

$$M_f + \sigma/C_M < T < M_s + \sigma/C_M. \tag{9}$$

The relationship between strain rate $\dot{\varepsilon}$ and $\dot{\theta}$ can be expressed as

$$\dot{\varepsilon} = -\frac{r\dot{\theta}}{l_0}, \tag{10}$$

where l_0 is the initial length of the wire, and r is the pulley's radius. Despite several assumptions in developing the Liang model, which is described by Eqs. (1) to (10), this model is complicated, making it difficult to use for designing a controller for an SMA actuator. This model requires various variables such as temperature and stress, in order to calculate the fraction of martensite. Additionally, this model has a high relative degree between the control input and the output, which causes extra complexity to the controller design process. Therefore, to address this issue, a nonlinear 1-degree-of-freedom model is considered for SMA-actuated manipulator as follows [16]:

$$I_z\ \ddot{\theta} + c\ \dot{\theta} + k\ \theta = \varphi\ u + h(\theta,\dot{\theta},u), \tag{11}$$

where $u = V^2$ is the control input, $h(\theta,\dot{\theta},u)$ is defined as the hysteretic nonlinear term, φ represents the unknown coefficient of the input. By considering $x = [\theta_1,\theta_2]^T = [\theta,\dot{\theta}]^T$ as the state variable, the state-space form of Eq. (11) can be defined as

$$\begin{aligned}\dot{\theta}_1 &= \theta_2,\\ \dot{\theta}_2 &= \frac{1}{I_z}[-k\ \theta_1 - c\ \theta_2 + \varphi\ u] + h(\theta_1,\theta_2,u).\end{aligned} \tag{12}$$

This state space model contains various unknown parameters, which are defined as $k = k_0 + \Delta k$, $c = c_0 + \Delta c$, and $\varphi = \varphi_0 + \Delta\varphi$, where k_0, c_0, and φ_0 are considered as known constants, while Δk, Δc, and $\Delta\varphi$ represent the unknown values. Therefore, Eq. (12) can be rewritten as follows:

$$\begin{aligned}\dot{\theta}_1 &= \theta_2,\\ \dot{\theta}_2 &= \frac{1}{I_z}[-k_0\ \theta_1 - c_0\ \theta_2 + \varphi_0\ u] - \Lambda(\theta_1,\theta_2) + h(\theta_1,\theta_2,u).\end{aligned} \tag{13}$$

where $\Lambda(\theta_1,\theta_2) = \frac{\Delta c}{I_z} + \frac{\Delta k}{I_z} - \frac{\Delta\varphi}{I_z}u$. By considering $y = \theta_1$ as the measurable output of the reduced-order model, the relative degree between input and output is found to be two, making the system well-defined. However, this system includes various sources of uncertainties such as the hysteretic nonlinear terms, un-modeled dynamics, and parametric uncertainties. To address this issue, the super twisting sliding mode control (ST-SMC) has been chosen as the control strategy due to its robustness against uncertainty.

B. Design of super-twisting sliding mode control

The nominal model of SMA according to Eq. (13) can be described as follows:

$$\begin{aligned}\dot{\theta}_1 &= \theta_2,\\ \dot{\theta}_2 &= \frac{1}{I_z}[-k_0\ \theta_1 - c_0\ \theta_2 + \varphi_0\ u].\end{aligned} \tag{14}$$

The sliding surface is defined as

$$s = \dot{e} + \alpha e, \tag{15}$$

in which α represents a positive value, and e is defined as the tracking error

$$e = \theta_d - \theta_1, \tag{16}$$

where θ_d represents the desired angular value. The time derivative of s in Eq. (15) gives

$$\dot{s} = \ddot{e} + \alpha\dot{e} = \ddot{\theta}_d - \ddot{\theta}_1 + \alpha\dot{e}. \tag{17}$$

Substituting Eq. (14) into Eq. (17) results in

$$\dot{s} = \ddot{\theta}_d - \frac{1}{I_z}[-k_0\ \theta_1 - c_0\ \theta_2 + \varphi_0\ u] + \alpha\dot{e}. \tag{18}$$

The control input u is comprised of two segments: the equivalent control law u_{eq} and the switching control law u_{sw},

$$u = \frac{I_z}{\varphi_0}[u_{eq} + u_{sw}], \tag{19}$$

where

$$u_{eq} = \ddot{\theta}_d + \frac{k_0}{I_z}\theta_1 + \frac{c_0}{I_z}\theta_2 + \alpha\dot{e}. \tag{20}$$

Also, the switching control law based on the super-twisting algorithm is expressed as follows:

$$u_{sw} = \beta\sqrt{|s|}\mathrm{sgn}(s) + w\int \mathrm{sgn}(s)\,dt, \tag{21}$$

where β and w are positive design values. Substituting Eqs. (20) and (21) into Eq. (19) gives

$$\begin{aligned}u = \frac{I_z}{\varphi_0}\Bigg[&\ddot{\theta}_d + \frac{k_0}{I_z}\theta_1 + \frac{c_0}{I_z}\theta_2 + \alpha\dot{e}\\ &+\beta\sqrt{|s|}\mathrm{sgn}(s) + w\int \mathrm{sgn}(s)\,dt\Bigg].\end{aligned} \tag{22}$$

In order to evaluate the stability of the closed loop system, the proposed control law (22), which is based on the nominal model, is applied to the actual model in Eq. (13). The resultant equation is used in rewriting Eq. (17) as

$$\dot{s} = -\beta\sqrt{|s|}\mathrm{sgn}(s) - w\int \mathrm{sgn}(s)dt + \Delta, \tag{23}$$

where $\Delta = \Lambda(\theta_1, \theta_2) - h(\theta_1, \theta_2, u)$. The Lyapunov function is defined as follows:

$$V(s) = \frac{1}{2}s^2. \tag{24}$$

By using Eq. (23), the time derivative of the Lyapunov function is expressed as follows:

$$\dot{V}(s) = s(-\beta\sqrt{|s|}\text{sgn}(s) - w\int \text{sgn}(s)\,dt + \Delta), \tag{25}$$

or

$$\dot{V}(s) \leq -\beta\sqrt{|s|}|s| - |s|\int w dt + |s|\Delta). \tag{26}$$

By considering $\Delta = \int \delta dt$, where $\delta = \dot{\Delta}$, Eq. (26) can be rewritten as follows:

$$\begin{aligned}\dot{V}(s) &\leq -\beta\sqrt{|s|}|s| - |s|\int w dt + |s|\int \delta dt,\\ &\leq -\beta\sqrt{|s|}|s| - |s|\int (w-\delta) dt.\end{aligned} \tag{27}$$

The robust stability of the system under the proposed control input is satisfied when $w > \delta$ as indicated in Eq. (27), resulting in $\dot{V} < 0$ at all times.

IV. Results and Discussion

A. Simulation studies

In this section, by using the Matlab/Simulink environment, numerical simulations are conducted to evaluate the performance of the super-twisting sliding mode controller. The mathematical model described by Eqs. (1) to (10) is considered as the actual model for modeling the behavior of SMA-actuated robotic arm. However, the proposed controller is designed by using a reduced-order model with one degree of freedom. By consideration of a time-varying reference trajectory, the system's response to this trajectory is depicted in Fig. 3. The results indicate that the proposed controller has high accuracy in tracking a desired trajectory. However, there is an acceptable tracking error caused by the hysteresis effect and un-modeled dynamics.

B. Experimental results

The robot arm platform actuated with SMA is depicted in Fig. 4. The fabricated platform contains the HN3806 two-phase encoder for measuring angular displacement of the arm at a frequency of 50 Hz. The measured data is sent to the MATLAB software via serial communication to produce suitable voltage values. Because of practical limitation in the voltage applied to the SMA, the maximum control input is considered as $V_{\text{max}} = 12$.

Figure 5 illustrates the performance of the proposed controller in response to a time-varying reference trajectory. The results show that the proposed control method is effective in the presence of un-modeled dynamics and other uncertainties. According to Fig 5a, the early overshoot occurs because the SMA actuator requires time to undergo a shape transformation. After some times, the heated wire connected to the arm, rapidly converges towards the desired value.

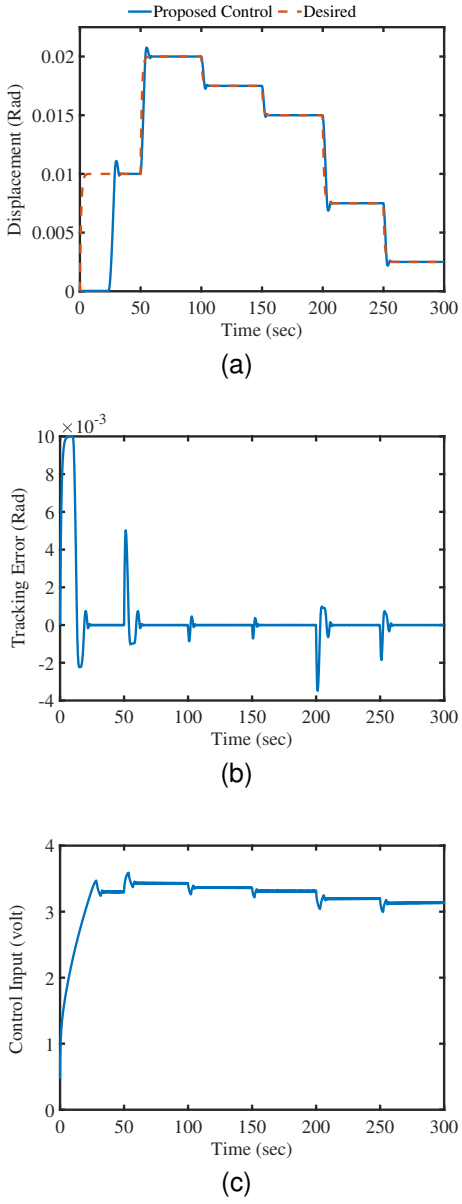

Fig. 3. The simulation results for the proposed controller in time-varying trajectory, (a) Displacement, (b) Tracking Error, (c) Control input.

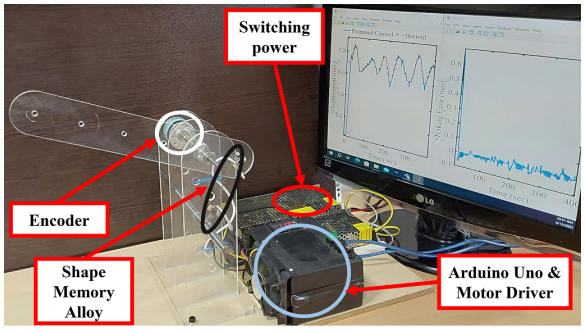

Fig. 4. The experimental setup.

To analyze the performance of the proposed controller

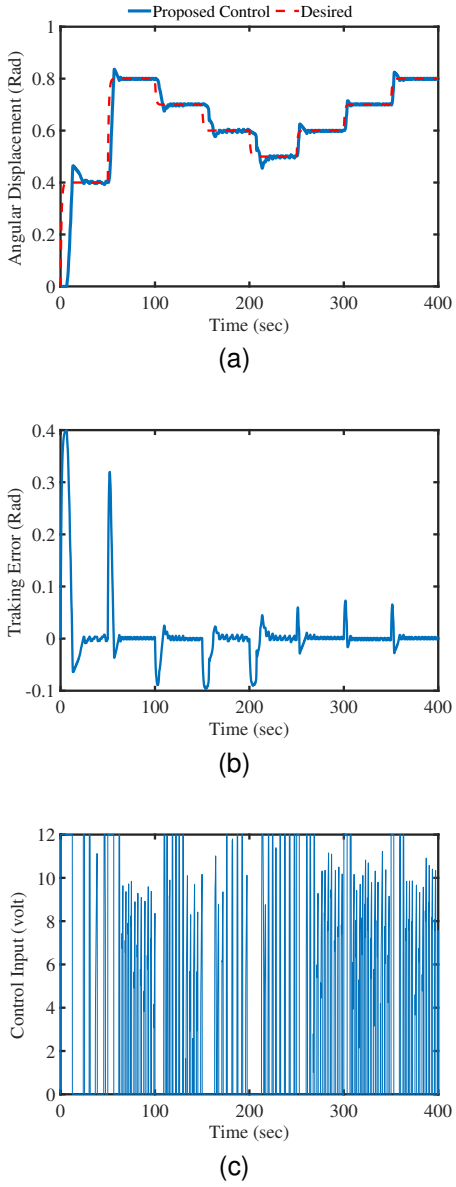

Fig. 5. The experimental results for the proposed controller in time-varying trajectory, (a) Displacement, (b) Tracking Error, (c) Control input.

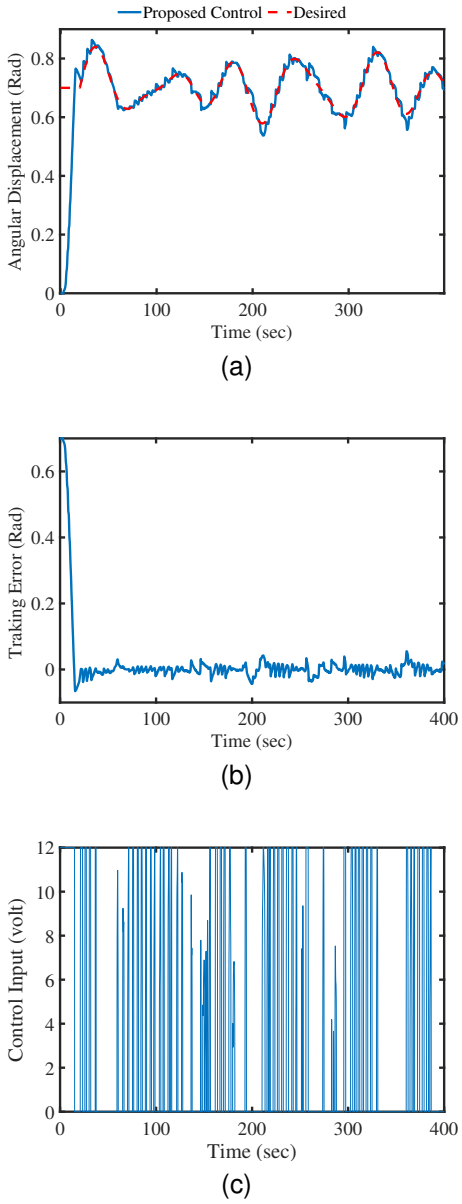

Fig. 6. The experimental results for the proposed controller in harmonic trajectory, (a) Displacement, (b) Tracking Error, (c) Control input.

TABLE I
THE RMS OF THE RESPONSES FOR HARMONIC TRAJECTORIES.

Reference Trajectory	**Proposed**		**SMC**	
	Tracking Error (Rad)	Control input (volt)	Tracking Error (Rad)	Control input (volt)
Harmonic	0.1084	5.5183	0.1321	6.010

across various trajectories, a harmonic reference trajectory is considered. The results in Fig. 6 illustrate that the proposed method, based on a 1-DOF model, has suitable performance in tracking the desired trajectory. To assess the performance of the proposed controller, the available results are compared with a conventional sliding mode controller. According to Fig. 7a, the performance of the proposed control in reducing the tracking error is much better than SMC. Moreover, the SMC exhibits higher chattering compared to the proposed method. To provide a comprehensive view, the root mean square (RMS) of the responses of the system is reported in Table I. The results highlight that the proposed control method has the ability to track the specified trajectory with higher accuracy and less control effort.

V. CONCLUSION

In this paper, a super-twisting sliding mode controller is designed for a robot arm actuated by SMA. A sensor for measuring angular displacement is attached to the platform. The effectiveness of the proposed control method is validated in different tests under various trajectories. The results show

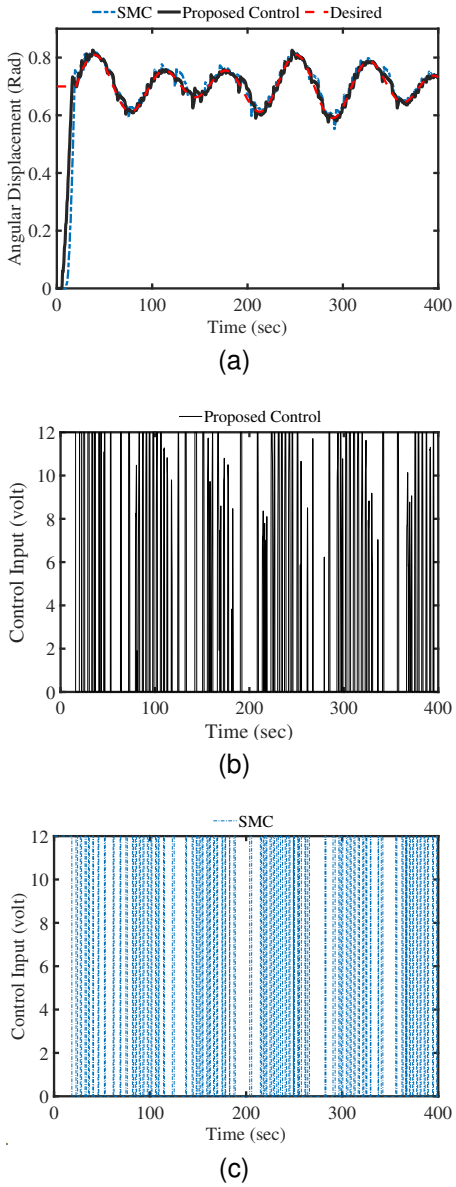

Fig. 7. The experimental comparative results for the proposed controller and SMC in harmonic trajectory, (a) Displacement, (b) Control input for the proposed method, (c) Control input for the SMC.

that the proposed control method robustly tracks the specified trajectories under model uncertainties .

REFERENCES

[1] Lee, J., M. Jin, and K.K. Ahn, "Precise tracking control of shape memory alloy actuator systems using hyperbolic tangential sliding mode control with time delay estimation," Mechatronics, 2013, 23(3), 310-317.

[2] Kode, V.R.C. and M.C. Cavusoglu, "Design and Characterization of a Novel Hybrid Actuator Using Shape Memory Alloy and DC Micromotor for Minimally Invasive Surgery Applications," IEEE/ASME Transactions on Mechatronics, 2007, 12(4), 455-464.

[3] Nair, V.S. and R. Nachimuthu, "The role of NiTi shape memory alloys in quality of life improvement through medical advancements: A comprehensive review," Proceedings of the Institution of Mechanical Engineers, Part H: Journal of Engineering in Medicine, 2022, 236(7), 923-950.

[4] Saito, T., T. Kagiwada, and H. Harada, "Development of an Earthworm Robot with a Shape Memory Alloy and Braided Tube," Advanced Robotics, 2009, 23(12-13), 1743-1760.

[5] Rodrigue, H., et al., "An overview of shape memory alloy-coupled actuators and robots," Soft Robotics, 2017, 4(1), 3-15.

[6] Williams, E.A., G. Shaw, and M. Elahinia, "Control of an automotive shape memory alloy mirror actuator," Mechatronics, 2010, 20(5), 527-534.

[7] Tai, N.T. and K.K. Ahn, "Adaptive proportional–integral–derivative tuning sliding mode control for a shape memory alloy actuator," Smart Materials and Structures, 2011, 20(5), 055010.

[8] Lagoudas, D.C., "Shape memory alloys: modeling and engineering applications," 2008, Springer.

[9] Lee, C.J. and C. Mavroidis. "Analytical dynamic model and experimental robust and optimal control of shape-memory-alloy bundle actuators."

[10] Zhang, D., et al., "Active modeling and control for shape memory alloy actuators," IEEE Access, 2019, 7, 162549-162558.

[11] Elahinia, M.H. and H. Ashrafiuon, "Nonlinear Control of a Shape Memory Alloy Actuated Manipulator," Journal of Vibration and Acoustics, 2002, 124(4), 566-575.

[12] Gilardi, G., E. Haslam, V. Bundhoo, and E.J. Park, "A shape memory alloy based tendon-driven actuation system for biomimetic artificial fingers, part II: modelling and control," Robotica, 2010, 28(5), 675-687.

[13] Tabrizi, V.A. and M. Moallem. "Nonlinear Position Control of Antagonistic Shape Memory Alloy Actuators," in 2007 American Control Conference, 2007.

[14] Nguyen, B.K. and K.K. Ahn, "Feedforward Control of Shape Memory Alloy Actuators Using Fuzzy-Based Inverse Preisach Model," IEEE Transactions on Control Systems Technology, 2009, 17(2), 434-441.

[15] Romano, R. and E.A. Tannuri, "Modeling, control and experimental validation of a novel actuator based on shape memory alloys," Mechatronics, 2009, 19(7), 1169-1177.

[16] Tai, N.T. and K.K. Ahn, "Output Feedback Direct Adaptive Controller for a SMA Actuator With a Kalman Filter," IEEE Transactions on Control Systems Technology, 2012, 20(4), 1081-1091.

[17] Tai, N.T. and K.K. Ahn, "Output Feedback Direct Adaptive Controller for a SMA Actuator With a Kalman Filter," IEEE Transactions on Control Systems Technology, 2012, 20(4), 1081-1091.

[18] Jin, M., J. Lee, P.H. Chang, and C. Choi, "Practical nonsingular terminal sliding-mode control of robot manipulators for high-accuracy tracking control," IEEE Transactions on Industrial Electronics, 2009, 56(9), 3593-3601.

[19] Utkin, V.I., "Sliding modes in control and optimization," 2013, Springer Science Business Media.

[20] Kamal, S., et al., "Continuous terminal sliding-mode controller," Automatica, 2016, 69, 308-314.

[21] Lee, H. and V.I. Utkin, "Chattering suppression methods in sliding mode control systems," Annual Reviews in Control, 2007, 31(2), 179-188.

[22] Ho, H.F., Y.-K. Wong, and A.B. Rad, "Adaptive fuzzy sliding mode control with chattering elimination for nonlinear SISO systems," Simulation Modelling Practice and Theory, 2009, 17(7), 1199-1210.

[23] Al-Dujaili, A.Q., et al., "Optimal super-twisting sliding mode control design of robot manipulator: Design and comparison study," International Journal of Advanced Robotic Systems, 2020, 17(6), 1729881420981524.

[24] Humaidi, A.J. and A.F. Hasan, "Particle swarm optimization–based adaptive super-twisting sliding mode control design for 2-degree-of-freedom helicopter," Measurement and Control, 2019, 52(9-10), 1403-1419.

[25] Elahinia, M.H. and H. Ashrafiuon, "Nonlinear control of a shape memory alloy actuated manipulator," J. Vib. Acoust., 2002, 124(4), 566-575.

[26] Liang, C. and C.A. Rogers, "One-Dimensional Thermomechanical Constitutive Relations for Shape Memory Materials," Journal of Intelligent Material Systems and Structures, 1997, 8(4), 285-302.